Available online at www.sciencedirect.com

ScienceDirect

Ceramics International 37 (2011) 1507–1514

CERAMICS INTERNATIONAL

www.elsevier.com/locate/ceramint

# Mechanochemical synthesis and characterisation of $BaTa_2O_6$ ceramic powders

Mustafa İlhan [a], Ayhan Mergen [a,*], Cemalettin Yaman [b]

[a] Department of Metallurgical and Materials Engineering, Marmara University, Göztepe Campus, 34722 Kadiköy, İstanbul, Turkey
[b] Department of Metallurgical and Materials Engineering, Yıldız Technical University, 34220 Davutpaşa, İstanbul, Turkey

Received 15 November 2010; received in revised form 1 December 2010; accepted 5 January 2011
Available online 3 February 2011

## Abstract

Mechanochemical synthesis was used to prepare $BaTa_2O_6$ powders from $BaCO_3$ and $Ta_2O_5$ precursors in a planetary ball mill. Effect of milling time and heat treatment temperature on the formation of $BaTa_2O_6$ and on the microstructure was investigated. Intensive milling of starting materials resulted in crystallization of $BaTa_2O_6$ even after 1 h of milling time and single phase $BaTa_2O_6$ was obtained after 10 h of milling under optimal conditions. The powder derived from 10 h of mechanical activation had crystallite size of 22 nm. But the increase in milling time did not decrease the crystallite size further. High energy milling activated the powders that although 1 h of milling led to formation of single phase $BaTa_2O_6$ at 1200 °C, this temperature decreased to 900 °C after 5 h of milling. No significant grain growth was observed when the milled powders were heat treated below 900 °C. However, annealing at 1100 and 1200 °C gave an average $BaTa_2O_6$ grain size of 180 and 650 nm, respectively. An unidentified phase started to form at 1100 °C increasing to high amounts at 1200 °C and they had different shapes and sizes than $BaTa_2O_6$ grains. These elongated large grains were thought to be due to liquid phase formation caused by iron contamination.

*Keywords:* B. X-ray method; $BaTa_2O_6$; Mechanosynthesis

## 1. Introduction

Mechanochemical synthesis is used effectively to produce advanced ceramic materials at nano scale [1]. In this technique, the reaction is activated by mechanical energy instead of heat energy required during the solid-state reaction. Mechanical alloying was invented at INCO's Paul D. Merica Research Laboratory around 1966 and was originally devised for synthesizing alloys and intermetallics [2,3]. The initial attempt was to develop an oxide dispersion strengthened nickel based super alloy [2]. However, nowadays it has been successfully used to synthesize a wide range of nanosized ceramic powders from structural parts to magnetic or electronic applications. Table 1 gives some mechanochemically synthesized ceramic materials with milling conditions and crystallite size. Mechanochemical synthesis mechanically activates the solid-state reactions in a ball mill and improves the sinterability of the ceramic precursors because mechanochemical activation supplies the part of the energy necessary to produce the chemical reaction. It has a number of advantages over the conventional ceramic processing techniques like high degree of homogeneity, lower sintering temperatures without calcination step, lower particle size and improved properties.

$BaTa_2O_6$ ceramic forms in $BaO–Ta_2O_5$ system and it has three polymorphs: orthorhombic, tetragonal, and hexagonal [12,13]. Orthorhombic is a low temperature form, tetragonal with a tungsten bronze type structure is an intermediate form and hexagonal is a high temperature form. These crystal structures can be described in terms of layers of corner- and edge-connected $TaO_6$ octahedra with Ba atoms occupying different types of tunnels parallel to the short axis [14]. These different polymorphs strongly affect the properties of $BaTa_2O_6$. The photocatalytic activity for water splitting and photoluminescence properties of $BaTa_2O_6$ were found to depend on the crystal form of $BaTa_2O_6$ that the order of the activities of the $BaTa_2O_6$ photocatalyst is higher for orthorhombic than tetragonal or hexagonal [15]. The dielectric properties of $BaTa_2O_6$ ceramic have been reported by several authors. Ichinose and Shimada [16] reported that $BaTa_2O_6$ ceramic has a

---

* Corresponding author. Tel.: +90 216 348 02 92x603;
fax: +90 216 345 01 26.
*E-mail address:* ayhan.mergen@marmara.edu.tr (A. Mergen).

0272-8842/$36.00 © 2011 Elsevier Ltd and Techna Group S.r.l. All rights reserved.
doi:10.1016/j.ceramint.2011.01.006

Table 1
Some examples of ceramic materials produced by mechanochemical method.

| | Application area | Milling type | Milling time | Crystallite size | Ref. |
|---|---|---|---|---|---|
| $Al_2O_3$/Nb nanocomposites | Structural | Planetary | 15 h | 8 nm (for Nb)<br>10 nm (for $Al_2O_3$) | [4] |
| $B_4C$ | Structural | Planetary | 80 h | 10–80 nm (TEM) | [5] |
| $BaTiO_3$–Ni | Ferroelectric | Planetary | 8 h | 28.4 nm (for $BaTiO_3$)<br>30.3 nm (for Ni) | [6] |
| $0.4Bi(Zn_{1/2}Ti_{1/2})O_3–0.6PbTiO_3$ | Ferroelectric | Planetary | 15 h | ~12 nm | [7] |
| $CePO_4$ | Protective coatings | Vibrating grinder | 15 min | ~12 nm | [8] |
| $LaGaO_3$ | Electrolyte | | 34 h | 20 nm | [9] |
| $(Pb_{0.4}Ca_{0.6})(Fe_{0.5}Ta_{0.5})O_3$ | Microwave dielectric | Spex | 60 h | 7.1 nm | [10] |
| $MgTa_2O_6$ | Microwave dielectric | Planetary | 8 h | 28 nm | [11] |

permittivity of 70, $Q_f$ (THz) of 2.1 and temperature coefficient of resonant frequency of +200 ppm/°C.

$BaTa_2O_6$ ceramic powder is produced by different techniques in the literature. Kato and Kudo [14] produced $BaTa_2O_6$ powder using $BaB_2O_4$ flux. The powder contained mostly orthorhombic phase with a small amount of the tetragonal phase. The hexagonal phase of $BaTa_2O_6$ was obtained by phase transition at 1720 K of the low-temperature forms. Conventional solid-state method forms $BaTa_2O_6$ phase at 1000 °C after prolonged heating time of 24 h [17]. $BaTa_2O_6$ was also produced by coprecipitation technique [17]. Barium and tantalum ions were precipitated by a mixture of ammonium oxalate and ammonium hydroxide. Single phase $BaTa_2O_6$ powder with an average particle size of 70 nm was produced after heat treatment at 750 °C for 6 h.

In this study, formation of $BaTa_2O_6$ ceramic powder was investigated by means of mechanochemical synthesis. Effect of milling time and annealing temperature on the formation of $BaTa_2O_6$ was examined in detail using XRD and SEM.

## 2. Experimental

Commercially available $BaCO_3$ (Fluka, 98.5%) and $Ta_2O_5$ (Alfa Aesar, 99%) powders were used as starting materials to produce $BaTa_2O_6$. Starting powders were initially homogenized by hand mixing in an agate mortar and placed in a stainless-steel vial (500 ml), with seven 20 mm stainless-steel balls (each of ball is 35 g in mass). Mechanical activation was carried out in a planatery ball mill (Fritsch Pulverisette 5) operating at 280 rpm with ball-to-powder ratio of 40:1 in air atmosphere for several times ranging from 1 to 20 h. The milled powder was annealed for 5 h at temperatures from 900 °C to 1200 °C in air. Phase composition of the milled and annealed powders was determined by X-ray powder diffractometer (XRD, Rigaku Corp., D-Max 2200) using Cu Kα radiation. The average crystallite sizes of the milled powders were determined using the Scherrer Formula [18]:

$$D = \frac{k \cdot \lambda}{B \cdot \cos\theta}$$

where $D$ is a mean particle size (nm); $k$ is a constant (taken as 0.9); $\lambda = 0.15406$, the wavelength of CuKα; $B$ is the full width at half maximum (rad); $\theta$ is the angle between incident and diffracted beams (°). The powder morphology after high energy milling was characterised using scanning electron microscopy (SEM, JEOL Ltd., JSM-5910LV) equipped with Energy Dispersive Spectrometer (EDS, OXFORD Industries INCAx-sight 7274).

## 3. Results and discussion

$BaCO_3$ and $Ta_2O_5$ were mixed as stoichiometric mixture according to the following reaction to produce $BaTa_2O_6$ powder.

$$BaCO_3 + Ta_2O_5 \rightarrow BaTa_2O_6 + CO_2$$

Fig. 1 shows the XRD patterns of powder mixture as-received and after different milling times. Even after 1 h of mechanochemical treatment $BaTa_2O_6$ phase started to form but

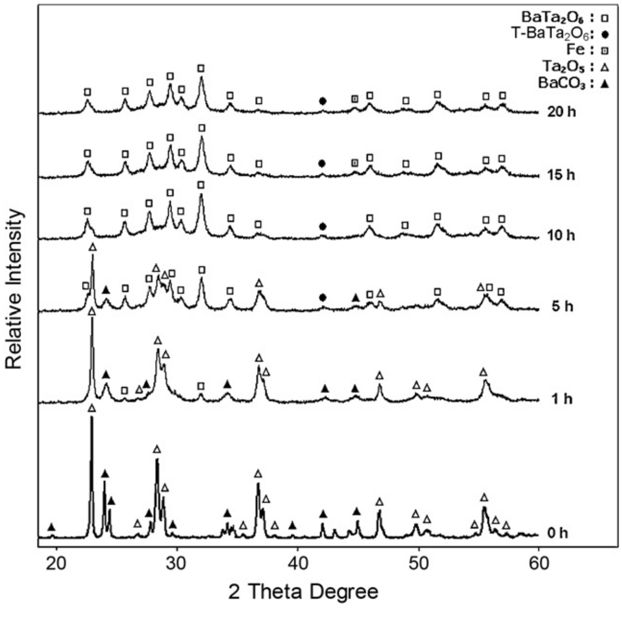

Fig. 1. X-ray diffraction patterns of barium carbonate and tantalum oxide mixture before high energy milling (0 h) and after milling for different times. T-$BaTa_2O_6$: Tetragonal with a tungsten bronze type structure.

Table 2
Crystallite size of mechanochemically milled $BaTa_2O_6$ powders.

| | $BaTa_2O_6$ crystallite size (nm) |
|---|---|
| 1 h of milling | 24 |
| 5 h of milling | 25 |
| 10 h of milling | 22 |
| 15 h of milling | 22 |
| 20 h of milling | 23 |

its content was very low. As milling time increased to 5 h, the intensity of $Ta_2O_5$ and $BaCO_3$ peaks decreased while the intensity of $BaTa_2O_6$ peaks increased. However, single phase $BaTa_2O_6$ structure was obtained after 10 h of milling where no $Ta_2O_5$ and $BaCO_3$ peaks were observed. This result reveals that mechanical energy during milling speed up the reaction between $BaCO_3$ and $Ta_2O_5$. XRD revealed that $Ta_2O_5$ and $BaCO_3$ remained crystalline after high energy milling but the peaks became broader and less intense markedly with milling time due to amorphization and refinement in crystallite size, which was measured by Scharrer's equation. The crystallite size of $BaTa_2O_6$ powder was around 25 nm after 5 h of milling (Table 2). The crystallite size was 22 nm after 10 h of high energy milling and did not change significantly with milling time that only decreased to 22–23 nm after 15 h and 20 h of

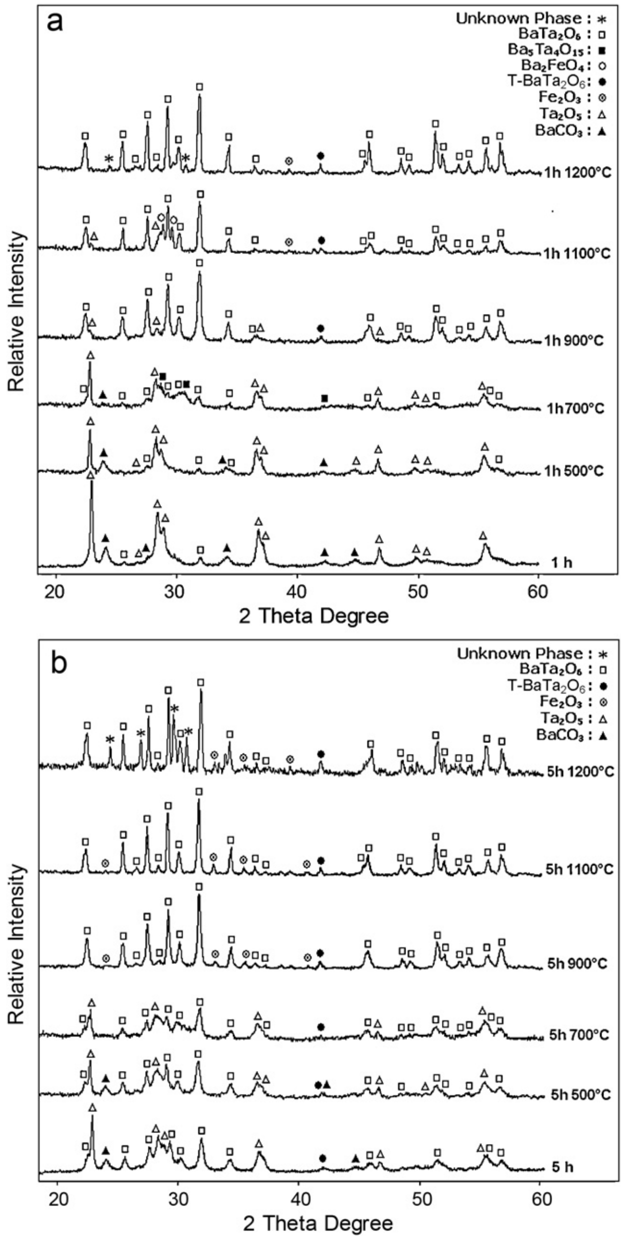

Fig. 2. X-ray diffraction patterns of powders heat treated at various temperatures for 5 h after mechanochemical treatment for (a) 1 h and (b) 5 h. T-$BaTa_2O_6$: Tetragonal with a tungsten bronze type structure.

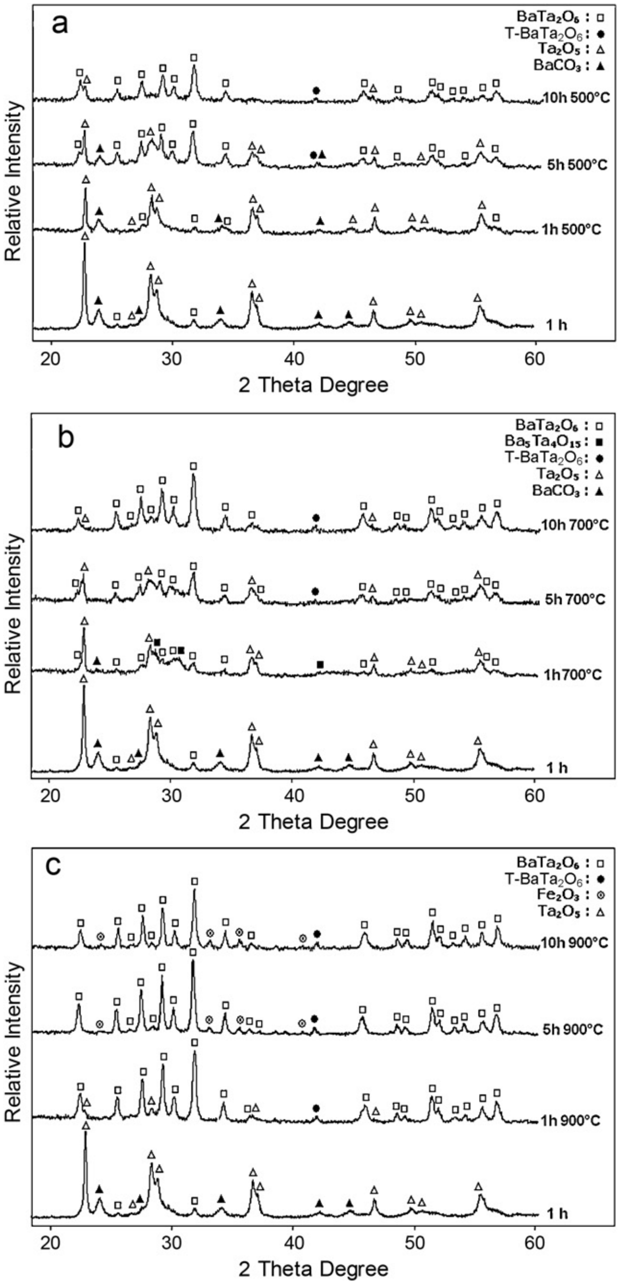

Fig. 3. X-ray diffraction patterns of powders heat treated at (a) 500 °C, (b) 700 °C and (c) 900 °C after mechanochemical treatment of 1 h, 5 h and 10 h. T-$BaTa_2O_6$: Tetragonal with a tungsten bronze type structure.

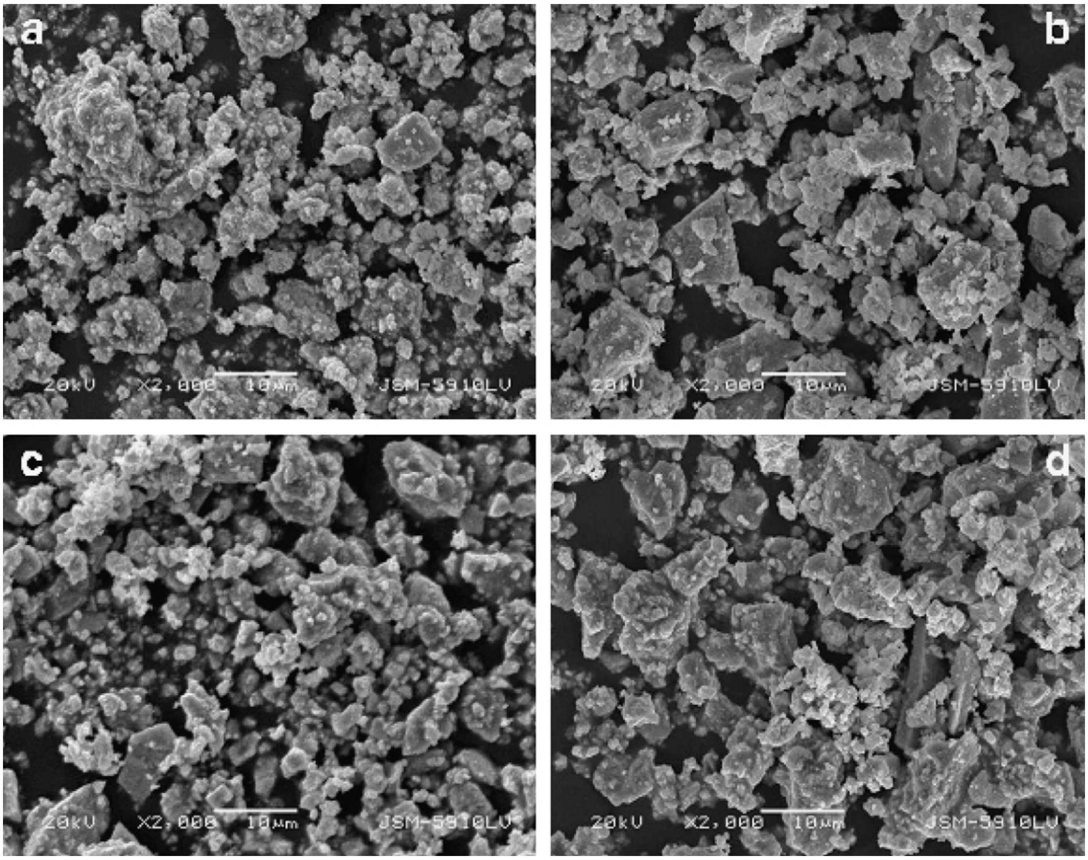

Fig. 4. SEM micrographs of powders milled for different times (a) 1 h, (b) 5 h, (c) 10 h, and (d) 15 h.

millings. Prolonging milling of $BaTa_2O_6$ broadened and lowered the intensities of the $BaTa_2O_6$ peaks which indicates that excessive milling decreased the crystallite size, led to defects and amorphous structure [11,7]. Iron related phases were also observed in XRD after 15 h of milling due to contamination.

In order to determine the effect of annealing temperature on the phase development and crystallinity of the milled powder, $BaCO_3$ and $Ta_2O_5$ powders milled for 1 h and 5 h were heat treated between 500 and 1200 °C for 5 h. The main phases were $BaCO_3$ and $Ta_2O_5$ and only a minor amount of $BaTa_2O_6$ phase formed in powders milled for 1 h (Fig. 2a). Heat treatment temperature of 500 °C did not make any change on the XRD pattern of this powder but as the heat treatment temperature increased to 700 °C, the intensities of $BaTa_2O_6$ peaks increased while the intensity of tantalum oxide peaks decreased. Another phase of $Ba_5Ta_4O_{15}$ (JCPDS Card No.: 18-193) also appeared at 700 °C due to heat treatment. At 900 °C, nearly single $BaTa_2O_6$ phase formed but there was minor amount of $Ta_2O_5$ which was completely reacted with $BaCO_3$ at 1200 °C forming single phase $BaTa_2O_6$ structure. No iron oxide impurity phase due to contamination effect was detected at 500, 700 and 900 °C most probably due to amorphous nature of powder but it appeared at 1100 °C due to increase in crystallinity. Another iron related phase of $Ba_2FeO_4$ (JCPDS Card No.: 23-1022) also started to form at 1100 °C but disappeared at 1200 °C converting to iron oxide and barium tantalate. Although single phase $BaTa_2O_6$ structure was obtained at 1200 °C in powder milled for 1 h, heat treatment of 5 h milled powder gave single phase $BaTa_2O_6$ at much lower temperature, 900 °C (Fig. 2b). This clearly indicates that mechanochemical treatment speed up the $BaTa_2O_6$ formation. Although heat treatment of 5 h milled powder at 700 °C gave mostly $BaTa_2O_6$, there was also unreacted $Ta_2O_5$ which was converted completely to barium tantalate at 900 °C. The absence of $Ta_2O_5$ and the increased and sharpened diffraction peaks of $BaTa_2O_6$ at 900 °C indicate that the reaction of the remaining $Ta_2O_5$ and $BaCO_3$ has been completed. The crystallinity behaviour of the powders milled for 1 h and 5 h were identical. XRD peaks were broader at 500 °C and 700 °C but they were sharper at 900 °C showing that the crystallization of $BaTa_2O_6$ from an amorphous phase has been greatly increased and no any amorphous phase was left at 900 °C.

The effect of both heat treatment temperature and milling time on the crystallization of $BaTa_2O_6$ was studied by heat treating the samples milled for 1 h, 5 h and 10 h at different temperatures (Fig. 3). XRD patterns of 1 h milled powder clearly indicated that although only a minor amount of $BaTa_2O_6$ phase appeared at 500 and 700 °C, the major phases were $BaCO_3$ and $Ta_2O_5$. However, at 900 °C, the prominent phase

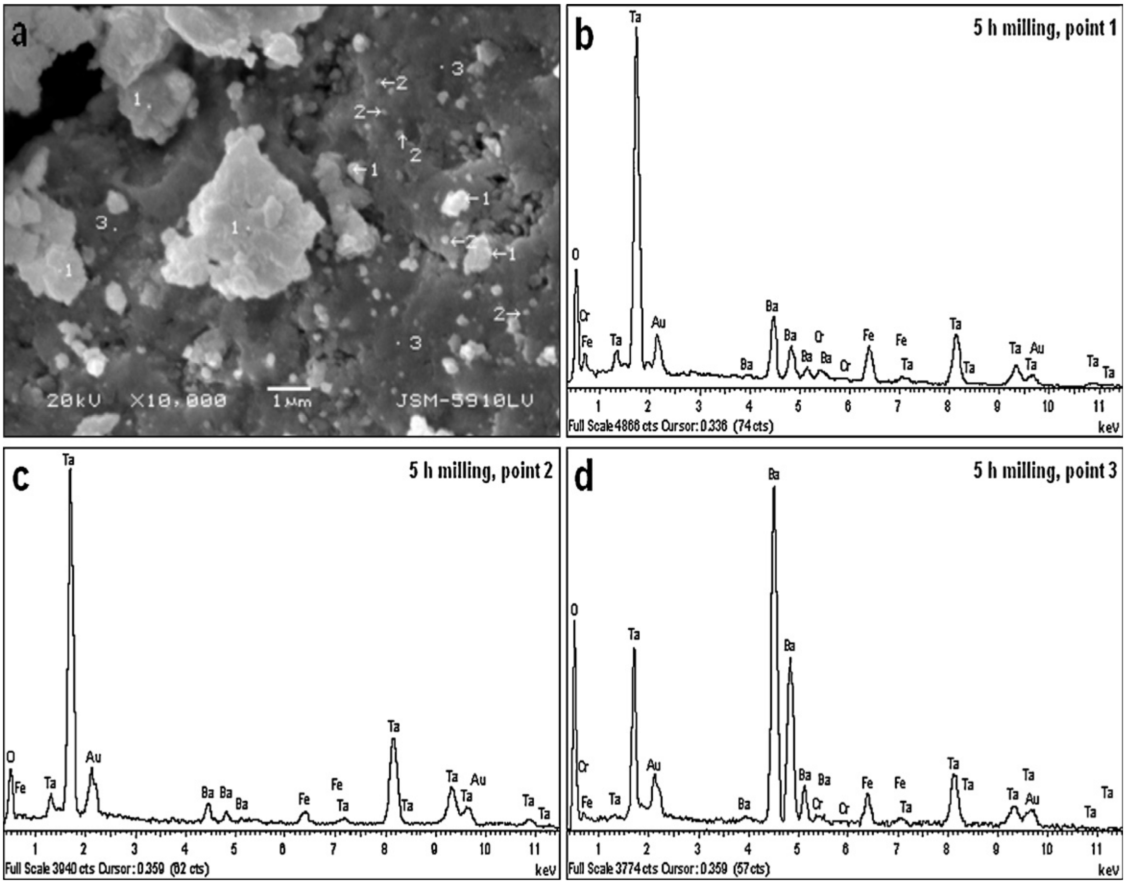

Fig. 5. SEM micrograph and EDS analysis of powders milled for 5 h (a) SEM micrograph at ×10,000 and EDS analysis of (b) $BaTa_2O_6$ phases (point 1), (c) Ta-rich or tantalum oxide phase (point 2) and (d) Ba-rich phase (point 3).

was $BaTa_2O_6$ and only a minor amount of $Ta_2O_5$ existed at this temperature. 5 h of high energy milling of $BaCO_3$ and $Ta_2O_5$ powders resulted in an increase in the amount of $BaTa_2O_6$ phase at 500 and 700 °C but there was still high amount of unreacted $Ta_2O_5$. Nevertheless, heat treatment temperature of 900 °C led to formation of single phase barium tantalate in 5 h milled powder. Longer milling time durations increased the content of $BaTa_2O_6$ phase at the same heat treatment temperatures. Although single phase $BaTa_2O_6$ was obtained at 700 and 900 °C, small amount of $Ta_2O_5$ was detected at 500 °C. These observations clearly imply that longer times of high energy milling and high heat treatment temperatures accelerates the formation of $BaTa_2O_6$ phase. Depending on the mechanochemical treatment time duration, crystallization temperature of the $BaTa_2O_6$ phase from an amorphous phase also varied. Although crystallization temperature was 900 °C for the 1 h and 5 h milled powder, it decreased to 500 °C when powder milled for 10 h (Fig. 3). It can be concluded that mechanochemical treatment time duration significantly decreases the crystallization temperature.

Fig. 4 shows the SEM micrographs of samples milled for different times. The microstructure of all samples was similar indicating that powders were agglomerated. However, the size of the agglomerates decreased with milling time until 10 h of milling. But the agglomerate sizes again started to increase at 15 h of milling time due to welding of particles. The particles within agglomerates were submicron in size and nearly spherical in shape. XRD analysis indicated that as the milling time increased, the content of barium tantalate phase also increased. SEM observation confirmed the XRD results. Fig. 5 gives the SEM micrographs of powders milled for 5 h together with EDS analysis. Three different particle compositions were observed: $BaTa_2O_6$ phase (point 1), Ta-rich or tantalum oxide phase (point 2) and Ba-rich phase (point 3). As the milling time increased $BaTa_2O_6$ phase content also increased. All three phases contained iron due to contamination effect. However, $BaTa_2O_6$ and Ba-rich phase contained higher amount of iron than the Ta-rich phase.

Effect of heat treatment temperature on the grain size and on the formation of phases was investigated at different temperatures. As can be seen from the SEM image in Fig. 6a, the powders had submicron rounded particles ranging between 60 and 125 nm after 5 h of milling. Low heat treatment temperatures of 500 and 900 °C did not cause a significant increase in grain size. $BaTa_2O_6$ grains had an average grains size of 120 and 180 nm at 500 and 900 °C, respectively. Although heat treatment at 1100 °C gave an average grain size of around 200 nm, which is near to 900 °C values, higher heat

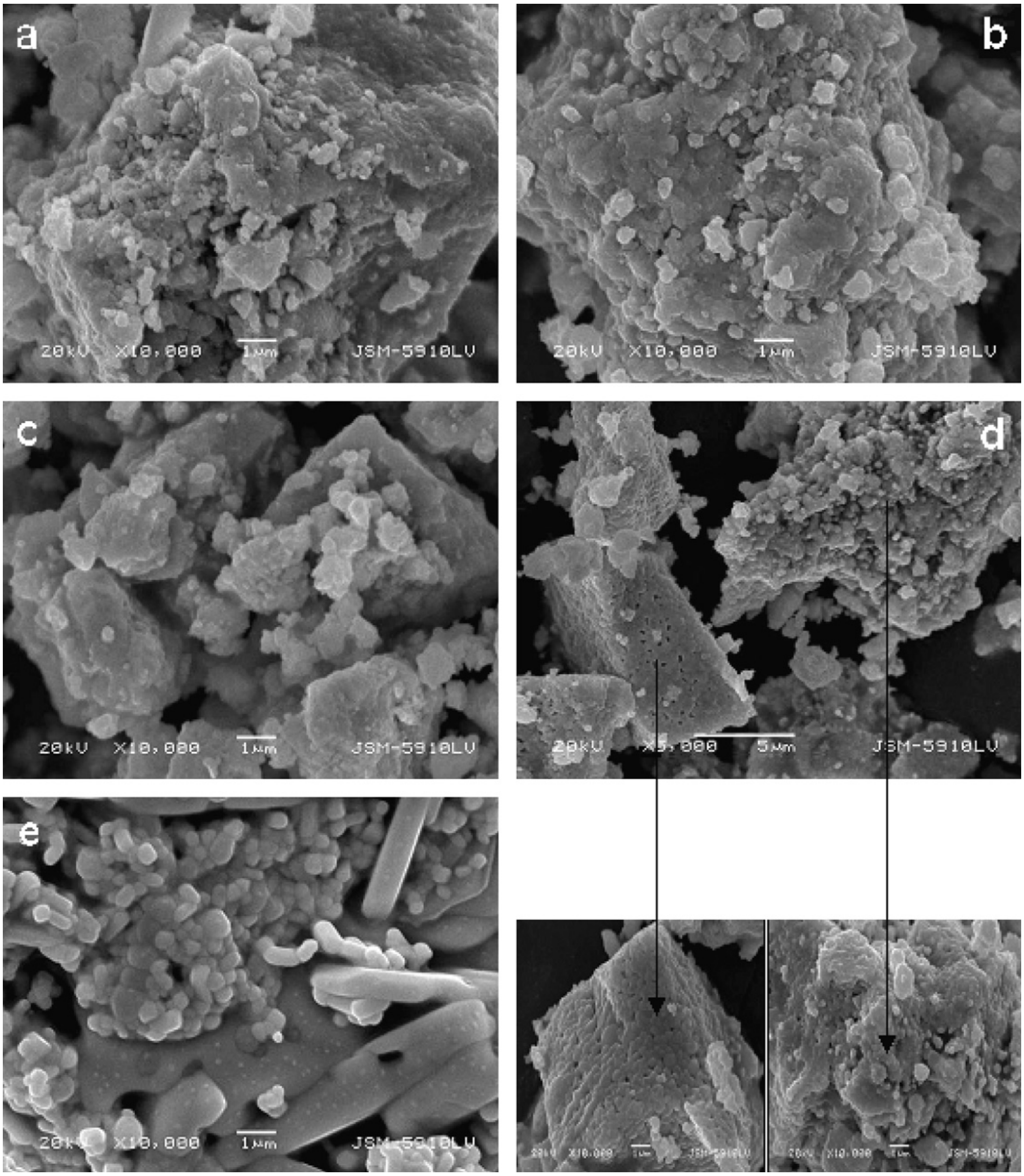

Fig. 6. SEM micrographs of powders milled for 5 h and heat treated at different temperatures for 5 h (a) as-milled, (b) 500 °C, (c) 900 °C, (d) 1100 °C, and (e) 1200 °C.

treatment temperature significantly increased the grain size reaching to an average value of 650 nm. In addition, another phase started to form at 1100 °C which was not detected in XRD possibly due to its low detection limit. The amount of this phase increased at 1200 °C and it was also observed by XRD but it could not be identified. SEM analysis of this unknown phase indicated that the grains of this phase were rounded in shape at 1100 °C but they were elongated at 1200 °C and although they were between 350 and 650 nm at 1100 °C, their sizes increased sharply at 1200 °C reaching 0.4–7 μm in thickness and 2.5–30 μm in length. The sharp increase in $BaTa_2O_6$ grain size and the larger size and elongated shape of unknown phase at 1200 °C were thought to be due to formation of a liquid phase. Fig. 7 confirms the results that the elongated grains were richer in Fe, which was due to contamination and formation of a liquid phase. Ba/Ta ratio of these grains was different from the ratio in Ba/Ta ratio in $BaTa_2O_6$. Therefore, these grains were thought to be unidentified phases observed in XRD. In addition, Fe-rich phases (point 3) were also detected in the microstructure that they formed as separate grains either between $BaTa_2O_6$ grains (point 1) or within the elongated grains (point 2). Formation of separate Fe phases at 1200 °C decreased the Fe content of $BaTa_2O_6$ and unknown phase at 1200 °C compared to the 1100 °C. Encapsulation of an iron-rich phase within elongated grains confirms the formation of an iron-related liquid phase.

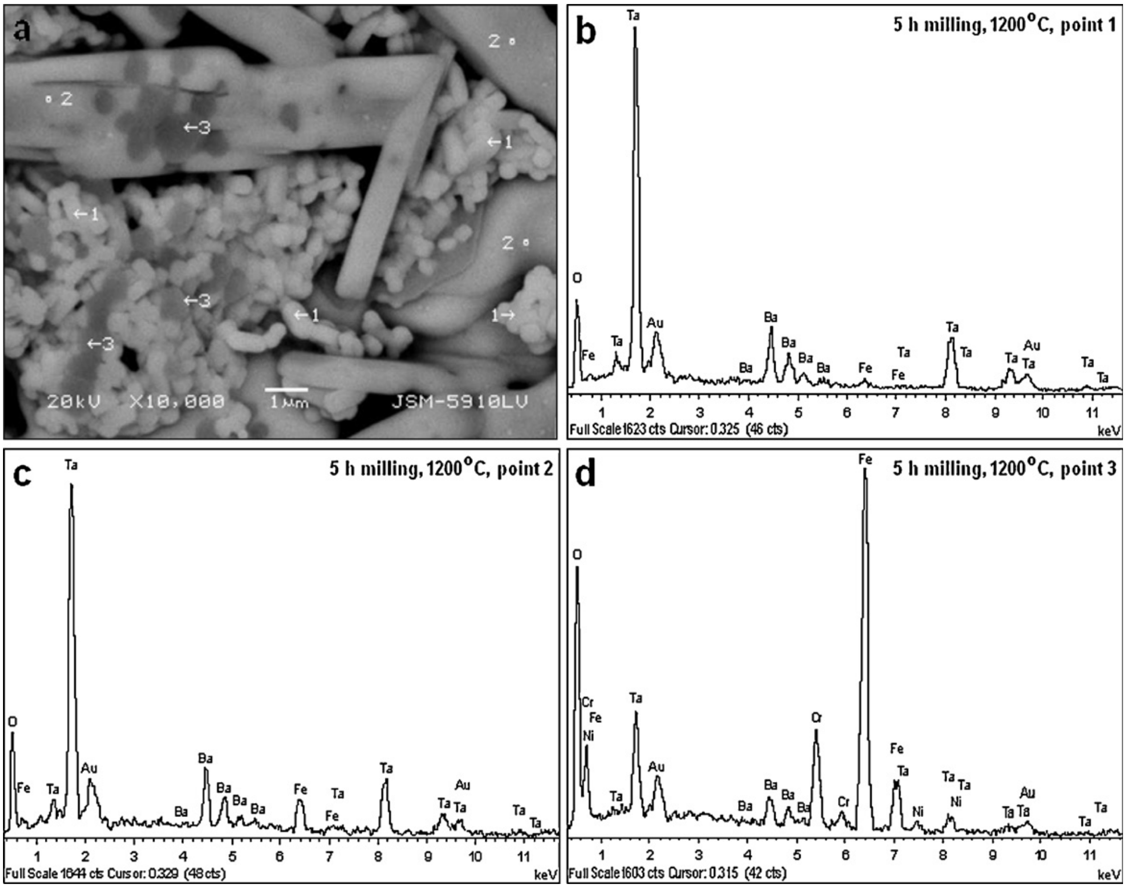

Fig. 7. SEM micrograph and EDS analysis of sample heat treated at 1200 °C for 5 h after 5 h of milling (a) back scatter image and EDS analysis of (b) $BaTa_2O_6$ grains (point 1), (c) Fe containing barium tantalate phase (point 2, elongated grains), and (d) Fe-rich phases (point 3).

## 4. Conclusions

Mechanosynthesis of $BaTa_2O_6$ phase was obtained after 10 h of milling in a planetary mill using $BaCO_3$ and $Ta_2O_5$ mixture. High energy milling speeded up the formation of $BaTa_2O_6$. Although $BaTa_2O_6$ phase started to form even after 1 h milling, single phase $BaTa_2O_6$ was formed after 10 h of milling time. Heat treatment of milled powder indicated that high energy milling activated the powder and led to formation of single phase at lower temperatures. XRD analysis indicated that an amorphous phase was produced after milling for 5 h, and a trace of $BaTa_2O_6$ crystallized from the amorphous phase. But significant crystallization of $BaTa_2O_6$ from the amorphous state was observed after annealing at 900 °C. Extended milling time decreased the single phase formation temperature of $BaTa_2O_6$. 10 h of high energy milling resulted in crystallite size of 22 nm. Low temperature annealing did not have almost any effect on the grain growth but increasing annealing temperature significantly increased the $BaTa_2O_6$ grain size. SEM examination indicated that although $BaTa_2O_6$ grains were below 1 μm at 1200 °C, elongated large grains (0.4–7 μm in thickness and 2.5–30 μm in length) with different compositions containing high iron formed due to liquid phase formation.

## Acknowledgement

We would like to give our great thanks to Yıldız Technical University Research Fund (Project No: 2011-07-02-DOP-03) for financial support of this investigation.

## References

[1] J. Beak, T. Isobe, M. Senna, Synthesis of pyrochlore-free $0.9Pb(Mg_{1/3}Nb_{2/3})O_3$–$0.1PbTiO_3$ ceramics via a soft mechanochemical route, Journal of the American Ceramics Society 80 (4) (1997) 973–981.

[2] L. Lu, M.O. Lai, Mechanical Alloying, first ed., Kluwer Academic Publishers, USA, 1998.

[3] J.S. Benjamin, Mechanical alloying, Scientific American 234 (1976) 40–49.

[4] H. Mostaan, M.H. Abbasi, F. Karimzadeh, Mechanochemical assisted synthesis of $Al_2O_3$/Nb nanocomposite by mechanical alloying, Journal of Alloys and Compounds 493 (2010) 609–612.

[5] E. Mohammad Sharifi, F. Karimzadeh, M.H. Enayati, Mechanochemical assisted synthesis of $B_4C$ nanoparticles, Advanced Powder Technology (2010).

[6] P.E. Sánchez-Jiménez, L.A. Pérez-Maqueda, M.J. Diánez, A. Perejón, J.M. Criado, Mechanochemical preparation of $BaTiO_3$–Ni nanocomposites with high dielectric constant, Composite Structures 92 (2010) 2236–2240.

[7] Q. Li, Z. Wang, Y. Yang, Mechanochemical synthesis and characterization of nanocrystalline $0.4Bi(Zn_{1/2}Ti_{1/2})O_3$–$0.6PbTiO_3$ powders, Materials Letters 63 (2009) 2297–2299.

[8] A. Matraszek, I. Szczygie, L. Macalik, J. Hanuza, Mechanochemical synthesis of cerium orthophosphate, Journal of Rare Earths 27 (2009) 598–602.

[9] A. Moure, A. Castro, J. Tartaj, C. Moure, Mechanosynthesis of perovskite $LaGaO_3$ and its effect on the sintering of ceramics, Ceramics International 35 (2009) 2659–2665.

[10] K.H. Yoona, H.S. Park, J.Y. Cho, E.S. Kim, Microwave dielectric properties of $(Pb_{0.4}Ca_{0.6})(Fe_{0.5}Ta_{0.5})O_3$ ceramics prepared by mechanochemical processing, Journal of the European Ceramic Society 23 (2003) 2579–2582.

[11] A. Mergen, Mechanochemical synthesis of $MgTa_2O_6$ ceramic, Ceramics International 35 (2009) 1151–1157.

[12] G.K. Layden, Polymorphism of $BaTa_2O_6$, Material Research Bulletin 2 (1967) 533.

[13] G.K. Layden, Dielectric and structure studies of hexagonal $BaTa_2O_6$, Material Research Bulletin 3 (1968) 349.

[14] H. Kato, A. Kudo, Photocatalytic water splitting into H-2 and O-2 over various tantalate photocatalysts, Catalysis Today 78 (2003) 561–569.

[15] H. Kato, A. Kudo, New tantalate photocatalysts for water decomposition into $H_2$ and $O_2$, Chemical Physics Letters 295 (1998) 487–492.

[16] N. Ichinose, T. Shimada, Effect of grain size and secondary phase on microwave dielectric properties of $Ba(Mg_{1/3}Ta_{2/3})O_3$ and $Ba([Mg,Zn]_{1/3}Ta_{2/3})O_3$ systems, Journal of the European Ceramic Society 26 (2006) 1755–1759.

[17] S.C. Navale, V. Samuel, A.B. Gaikwad, V. Ravi, A co-precipitation technique to prepare $BaTa_2O_6$, Ceramics International 33 (2007) 297–299.

[18] B.D. Cullity, S.R. Stock, Elements of X-ray Diffraction, third ed., Prentice Hall, USA, 2001.